Video Article

Application of High-speed Super-resolution SPEED Microscopy in Live Primary Cilium

Andrew Ruba[1], Wangxi Luo[1], Weidong Yang[1]

[1]Department of Biology, Temple University

Correspondence to: Weidong Yang at weidong.yang@temple.edu

Abstract

The primary cilium is a microtubule-based protrusion on the surface of many eukaryotic cells and contains a unique complement of proteins that function critically in cell motility and signaling. Since cilia are incapable of synthesizing their own protein, nearly 200 unique ciliary proteins need to be trafficked between the cytosol and primary cilia. However, it is still a technical challenge to map three-dimensional (3D) locations of transport pathways for these proteins in live primary cilia due to the limitations of currently existing techniques. To conquer the challenge, recently we have developed and employed a high-speed virtual 3D super-resolution microscopy, termed single-point edge-excitation sub-diffraction (SPEED) microscopy, to determine the 3D spatial location of transport pathways for both cytosolic and membrane proteins in primary cilia of live cells. In this article, we will demonstrate the detailed setup of SPEED microscopy, the preparation of cells expressing fluorescence-protein-labeled ciliary proteins, the real-time single-molecule tracking of individual proteins in live cilium and the achievement of 3D spatial probability density maps of transport routes for ciliary proteins.

Video Link

The video component of this article can be found at https://www.jove.com/video/56475/

Introduction

Since stated by Ernst Abbe in 1873, the resolution of conventional light microscopy has been believed to be limited to approximately 200 nm due to light diffraction from the objective[1,2]. Currently, super-resolution light microscopy techniques break this limitation and allow the capture of dynamic images with sub-diffraction (< 200 nm) resolution. The techniques generally fall into two broad categories: stimulated emission depletion (STED) microscopy based approaches, which generate sub-diffraction illumination volume due to nonlinear optical response of fluorophores in samples[3]; and photoactivated light microscopy (PALM) and stochastic optical reconstruction microscopy (STORM)-based super-resolution techniques, which utilize mathematical functions to localize the centroids of fluorophores and then reconstitute these centroids to form super-resolution images[4,5]. Currently, due to the relatively uncomplicated optical setup, PALM and STORM are extensively employed by only activating a small subset of fluorophores in each frame of a long video of a biological preparation. This allows for the more accurate localization by 2D Gaussian fitting of the fluorescent spot, termed the point spread function (PSF), of fluorescently-labeled proteins in each frame of the video. The 2D location of each fluorescently-labeled molecule can then be superimposed on a single imaging plane to produce a super-resolution image of the biological preparation[1,2]. While these single-molecule localization, super-resolution approaches to microscopy certainly revolutionized how imaging of biological samples was performed, there are still challenges to be overcome. For example, STORM and PALM can achieve their best spatial resolutions after fixation of biological samples and thus present a static representation of the fluorescently-labeled proteins, which is a similar limitation of electron microscopy. Additionally, to achieve high spatial resolution for each fluorescently-labeled protein in live cells, samples must be imaged at very long framerates which are unable to capture protein dynamics. Therefore, it is necessary to overcome these main technical hurdles.

To obtain a high spatiotemporal resolution that is well-suited for detecting fast-moving proteins or RNAs in live cells, we have developed super-resolution SPEED microscopy in our laboratory (**Figure 1**)[6,7,8]. Several major technical advances in SPEED microscopy have previously enabled us to successfully track nucleocytoplasmic transport of small molecules, proteins, mRNA and virus through native nuclear pore complexes (NPCs)[6,7,8]. Briefly, the following features of SPEED microscopy will be used to track fast-moving macromolecules through sub-micrometer rotationally symmetrical structures in live cells, such as NPCs and primary cilia: (**1**) An inclined or a vertical illumination PSF enables the excitation of single molecules within a small diffraction-limit volume in the focal plane (**Figure 1**); (**2**) The inclined PSF can greatly avoid out-of-focus fluorescence and thus improve the signal-to-noise ratio. (**3**) The optical density of 100-500 kW/ cm^2 in the illumination PSF allows thousands of photons to be collected from single fluorophores with fast detection speeds (> 500 Hz). (**4**) The fast detection speed also greatly reduces the single-molecule spatial localization error (< 10 nm) in determining the spatial trajectories of moving fluorescent molecules in live cells, because molecular diffusion is one of major factors causing imperfections of single-molecule localization for moving molecules. (**5**) Well-established 2D to 3D transformation algorithms enable us to provide 3D spatial probability density maps of transport routes for molecules in the NPC or the primary cilium. It is noteworthy that our conversion process between the Cartesian and the cylindrical coordination system is

used to generate a 3D spatial probability density map rather than 3D single-molecule tracking (**Figure 2**). Previously, electron microscopy data have revealed that the NPC[9,10] and the primary cilium[11] both have a rotationally symmetrical structure. In principle, randomly diffusing molecules moving through the NPC or primary cilium should also have rotationally symmetrical distributions. As shown in **Figure 2**, a high number of randomly diffusing molecules inside the cylinder would generate rotationally symmetrical distributions at the cross-section view as that in the NPC, further resulting in an approximately uniform spatial distribution within each very small sub-region between two neighboring rings (**Figure 2E**). This uniform distribution leads that the spatial distribution along θ dimension in the cylindrical system is constant. Then the 3D coordinates (R, X, θ) can be simplified to be the 2D coordinates (R, X, constant). Actually, our conversion process between the Cartesian and the cylindrical systems is from 2D (X, Y) to 2D (R, X, constant). The constant θ, refers to the spatial density *p* in **Figure 2E**, is calculated by using the equation $A_j = 2 * \sum_{i=j}^{n} \rho_i * s_{i,j}$.

Ultimately, single-molecule tracking has broad application in biological research, thus, it is natural that a plethora of techniques will be developed to fill specific biological niches[12,13,14]. Such is the case with SPEED microscopy. Previously, when coupled with a 3D transformation algorithm, this technique was developed to resolve 3D transport routes of transiting molecules through the NPCs, a sub-diffraction-sized and rotationally symmetric biological structure[6]. In this paper, primary cilia are shown to be excellent model organelles as well. Primary cilia are cylindrical, antenna-like organelles (~125 nm radius) that project from the surface of most mammalian cells[15,16,17]. They are responsible for receiving external signals and transmitting an intracellular response typically associated with growth and metabolism[15,16]. Therefore, flux of structural proteins, recycling of transmembrane receptors, and transmission of intracellular messengers are vital responsibilities of primary cilia. At the juncture between the primary cilia and the cell body is a critical selectivity barrier, called the transition zone or TZ, through which all this protein transport must occur[11,18,19,20]. In addition to the gating function of the TZ, at least two transport processes, intraflagellar transport and passive diffusion, are thought to be responsible for the movement of protein through this region[16,21,22]. From a human health standpoint, the loss of primary cilia and subsequent deregulation of downstream signaling is characteristic of many cancers. In addition, many genetic diseases, such as Bardet-Biedl syndrome and polycystic kidney disease, are associated with defective protein transport[23]. Both the sub-diffraction limit size and the complex process of selective protein transport through the TZ make the primary cilia a prime target for this technique. In this methods paper, we will demonstrate the tracking of a ciliary transmembrane protein, somatostatin receptor 3 (SSTR3)[24], labeled externally with Alexa Fluor 647 and a component of IFT, IFT20[25], labeled with a fused GFP molecule.

Protocol

1. NIH-3T3 cell preparation for SPEED microscopy from stock

1. 1.5 weeks in advance of the experiment, recover a fresh culture of NIH-3T3 cells from a frozen stock by thawing at 37 °C and transferring the cells to a 25 cm[2] cell culture flask with 3 mL of Dulbecco's Modified Eagle's Medium (DMEM) supplemented with 110 mg/mL sodium pyruvate, 2 mM glutamine, 10% fetal bovine serum, and 1% penicillin/streptomycin.
2. Incubate the cells at 37 °C in a 5% CO_2 incubator.
3. Split cells at 80% confluency, about every two days, at least three times before experimental day to ensure homogeneity of cell cycle. Trypsinize cells with 0.25% trypsin for 2 min at 37 °C, aspirate trypsin and replace it with 2 mL of medium. Pipette the medium repeatedly to break up cell clusters, remove the desired number of cells and bring total volume of media back up to 3 mL.
   NOTE: NIH-3T3 were previously genetically engineered to express NPHP-4, a protein that localizes to the TZ[26], fused at the C terminus to mCherry. mCherry is a fluorophore which can be excited with 561 nm illumination to quantitatively localize the TZ selectivity barrier and orient the primary cilia.
4. Two days before the experiment, plate the cells into a 35 mm glass bottom dish at 60-70% confluency with 1.5 mL of the same medium as step 1.1 and return the cells to the incubator.
5. One day before the experiment, chemically transfect the cells with the desired plasmid. Mix 500 - 1000 ng of the desired plasmid (see the **Note** below) in a 1:2.5 ratio with transfection reagent in 0.25 mL of reduced serum media without antibiotics for 30 min. Aspirate media from the 35 mm glass bottom dish and replace it with the 0.25 mL plasmid/transfection reagent mix plus an extra 1.25 mL of reduced serum media without antibiotics. Reduced serum media serves the purpose facilitating a successful transfection, inducing primary cilia growth, as well as keeping the cells alive long enough to perform experiment. Return cells to the incubator for the experiment on the following day.
   NOTE: When performing single-molecule tracking of IFT20, a plasmid containing a genetically-modified IFT20 fused at its C terminus to GFP is used[25]. When performing single-molecule tracking of SSTR3, a plasmid containing a genetically-modified SSTR3 fused at its N terminus to an acceptor peptide (AP) domain and C terminus to GFP is used[22]. In addition to the SSTR3 construct, a plasmid containing the biotin ligase BirA must be co-expressed and the transfection media must be supplemented with 10 µM biotin. BirA then attaches biotin to the AP domain of newly synthesized AP-SSTR3-GFP molecules at the level of the ER. Alexa647 conjugated to three of the four biotin-binding sites on streptavidin, on average, may then be supplemented to the media prior to imaging to fluorescently label the AP-SSTR3-GFP molecules on the external surface of the cell[22,27]. GFP and AlexaFluor647 are used in this method; however, other fluorescent probes can be used if they have similarly high photo-stability and quantum yield.
6. If using the externally-labeled SSTR3 construct, remove the media from the glass bottom dish 1 h before experiment, wash the cell 5 times with 1 mL of phosphate-buffered saline (PBS), and add 1 mL of reduced serum media supplemented with 1 µM Alexa647 conjugated streptavidin.
7. No more than 15 min before the experiment, remove media from the glass bottom dish and wash the transfected and labeled cells 5 times with 1 mL of PBS.
8. Place 1 mL of imaging buffer (20 mM HEPES, 110 mM KOAc, 5 mM NaOAc, 2 mM MgOAc, 1 mM EGTA, pH 7.3) in the glass bottom dish.
   NOTE: In the imaging buffer, cells are viable for no longer than 3 h. Therefore, only 2 h of experiments are performed on each dish.

2. SPEED microscopy

Note: The SPEED microscopy setup includes an inverted fluorescence microscope equipped with a 1.4-NA 100× oil-immersion apochromatic objective, a 35 mW 633 nm He-Ne laser, 50 mW solid state 488-nm and 561-nm lasers, an on-chip multiplication gain charge-coupled-device

camera and a microscope software package for data acquisition and processing (**Figure 1**). For individual channel imaging, GFP, mCherry, and Alexa647 are excited by 488 nm, 561 nm, or 633 nm lasers, respectively. For single molecule tracking, single point illumination is used to track individual fluorescently-labeled molecules. For epifluorescence imaging, a concave lens is placed in the laser illumination path to expand the beam into a uniform field of illumination. The fluorescence emissions are collected by the same objective, filtered by a dichroic filter (405/488/561/635) and an emission filter (405/488/561/635), and imaged with the above CCD camera operating at 500 Hz for single molecule tracking or 2 Hz for epifluorescence imaging.

1. Affix the glass bottom plate to the stage of the microscope and locate a cell that is properly expressing the desired constructs. Once a suitable cell has been found, align the NPHP4-mCherry spot at the base of the primary cilia with the location on the imaging plane that corresponds to the laser's single point illumination.
2. Capture an epifluorescence image of NPHP4-mCherry and either IFT20-GFP or AP-SSTR3-GFP using the "Snap" function in the "Camera" tab of the "Focus Controls" window if using the digital microscopy software package (see **Table of Materials**).
   NOTE: These images will act as a reference for the subsequent single molecule locations.
3. Once the reference images are obtained, locally reduce the concentration of labeled single molecules. Photo-bleach the TZ with 1 mW laser illumination for 20 s or until the fluorescence intensity is close to that of background fluorescence.
   NOTE: When the precise concentration can be controlled, 0.1-1 nM labeled single molecules are used.
4. To prepare for single molecule tracking, reduce the laser illumination power to ~0.15 mW for single molecules labeled with GFP or ~0.5 mW for molecules labeled with Alexa647.
5. As soon as the laser power and imaging parameters are set, maximum gain and intensification and 2 ms frame rate, for single molecule imaging, engage the appropriate illumination laser and record non-photobleached, labeled single molecules as they are transported through the photobleached region of the TZ by clicking the "Stream" button in the "Camera" tab of the "Focus Controls" window.
   NOTE: No more than 2 min of video should be captured to minimize the effects of ciliary drift to a negligible level.
6. After capturing the single molecule video, process the videos using a 2D Gaussian fitting algorithm, such as Glimpse by the Gelles Lab, which precisely localizes the centroid of each single molecule's excitation PSF in an encompassing area of interest (AOI).
7. Select all single molecule locations with precision <10 nm and correct the center of cilia based on distribution of single molecule locations fitted with a 2D Gaussian function.
   NOTE: By using 2D to 3D transformation algorithm, the 3D transport routes of IFT20-GFP and AP-SSTR3 routes are clearly shown on ciliary axonemal or ciliary membrane, respectively.

3. 2D to 3D Transformation

1. Once several thousand localizations for transiting molecules (signal to noise ratio > 11) in the cilium are collected, select the long axis of the cilium as the X-dimension. Make a Y dimension histogram of the locations and obtain the bin sums in 10 nm increments.
   NOTE: The 2D to 3D transformation may be evaluated by hand or any software or programming language. The authors have successfully implemented the transformation in both Matlab and Python 2.7.

Representative Results

This section demonstrates the data obtained from performing SPEED microscopy at the TZ of primary cilia to study the transport route of SSTR3 connected by a ~15 nm external linker to Alexa647 (**Figure 3A**). It serves the dual purpose of verifying the 3D transformation algorithm. Alexa647 should only label the external surface of the primary cilium and therefore, the 3D transport route should reveal a high-density transport route at that location. NIH-3T3 stably expressing NPHP3-mCherry at the TZ must be transfected with AP-SSTR3-GFP and incubated according to the above protocol with streptavidin-conjugated Alexa647. Wide field imaging of the mCherry label is used to localize the TZ while the GFP is used to ensure that a cell has expressed the desired SSTR3 construct. Additionally, wide field imaging of the Alexa647 label using 633 nm illumination is necessary to confirm that the cell has properly expressed the BirA plasmid and has absorbed sufficient biotin from the media. Positive confirmation is characterized by a visible cilium distinct from the background fluorescence (**Figure 3B**). Efficient labeling of the AP-SSTR3-GFP construct with streptavidin-conjugated Alexa647 can only occur under these conditions. Once positive confirmation of selective labeling of the primary cilium by Alexa647 has been obtained, photobleaching and single point illumination of the TZ with a 633 nm laser will allow single molecules to be visualized. Before data analysis, superimposing the single molecule video on the wide field illumination is a useful validation step (**Figure 3C**). For example, if the laser is not aligned properly, no single molecules will appear to co-localize with the TZ. Another pre-data analysis validation step to ensure an adequate signal-to-noise ratio is to check the intensity at the TZ over the length of the single molecule video (**Figure 3E**). Such analysis can be performed quickly in ImageJ using the 'plot z axis profile' function. The peaks in **Figure 3F** correspond to the appearance of a single molecule at the TZ with a signal-to-noise of ~5.0. This graph is also capable of ensuring that enough photobleaching has occurred as evidenced by the well-separated frequency of single molecules. **Figure 3G** demonstrates a low signal-to-noise ratio of < 0.5. One explanation would be that the laser is not aligned directly on the TZ. Another reason may be that the laser illumination power is too low. Both explanations result in low excitation and, therefore, low emission of the fluorophores at the TZ. After these checks have been made, 2D Gaussian fitting of the single molecules will produce their trajectories in the TZ (**Figure 3H**). Superimposing many trajectories will produce the transport route of the labeled protein of interest in the TZ (**Figure 3I**). Since the 2D Gaussian fitting corresponds to the pixel values on the detector, the x, y single molecule data may be merged with the wide field image of the TZ and primary cilia to further illustrate the protein of interest's localization (**Figure 3J**).

IFT20 is a component of the IFT complex, which carries cargo along microtubules inside primary cilia[25]. Arl13b-mCherry, a widely used ciliary marker protein was used to label primary cilia[19]. Wide-field epi-fluorescence microscopy was used to image the primary cilium expressing both Arl13b-mCherry and IFT20-GFP and then switched to SPEED microscopy to track individual IFT20-GFP proteins in primary cilia after a pre-photobleaching of GFP fluorescence down to single-molecule level in the illumination area of SPEED microscopy (**Figure 4A-4C**).

Eventually, hundreds of single-molecule IFT20-GFP locations with a systematical localization precision of < 16 nm can be obtained from the primary cilium of a live cell (**Figure 4D**). According to our simulation, 250 single molecule locations with a radius of 95 nm was enough to generate a reliable 3D transport route (**Figure 5**). A final determination of IFT20-GFP transport route is based on thousands of single-molecule IFT20-GFP locations collected from ten cilia (**Figure 4E**). Since primary cilia possess a structure with rotational symmetry, the 2D to 3D transformation algorithm was applied to the 2D projected data. Interestingly, the 3D spatial probability density maps of IFT20 indicated that only a single high-density region with a ~60-nm width peaked at ~95 nm along the radius of primary cilia (**Figure 4E**). This high-density region likely co-localizes with the axonemal microtubules, in agreement with the known location of the IFT route (**Figure 4F**).
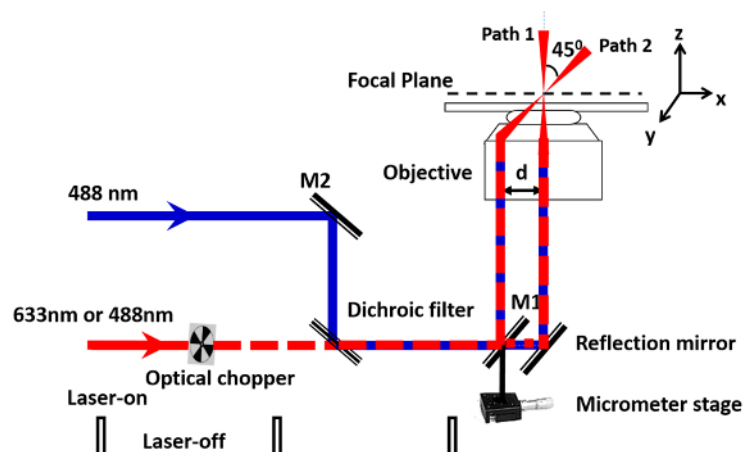

Figure 1. Simplified schematic of SPEED Microscopy. A vertical (path 1) or an inclined (path 2) point spread function is used to illuminate single fluorophore molecules in the focal plane. "d" refers to the distance between vertical illumination laser beam which passes through the center of the objective and angled illumination which is achieved by focusing the illumination laser on the edge of the objective. Two or more lasers regulated by an optical chopper to have an on-off excitation mode are used to track the single molecules transiting through the NPC or the primary cilium. The off time is at least ten-fold longer than the photobleaching time of the fluorophore label on the targeted molecules. Please click here to view a larger version of this figure.
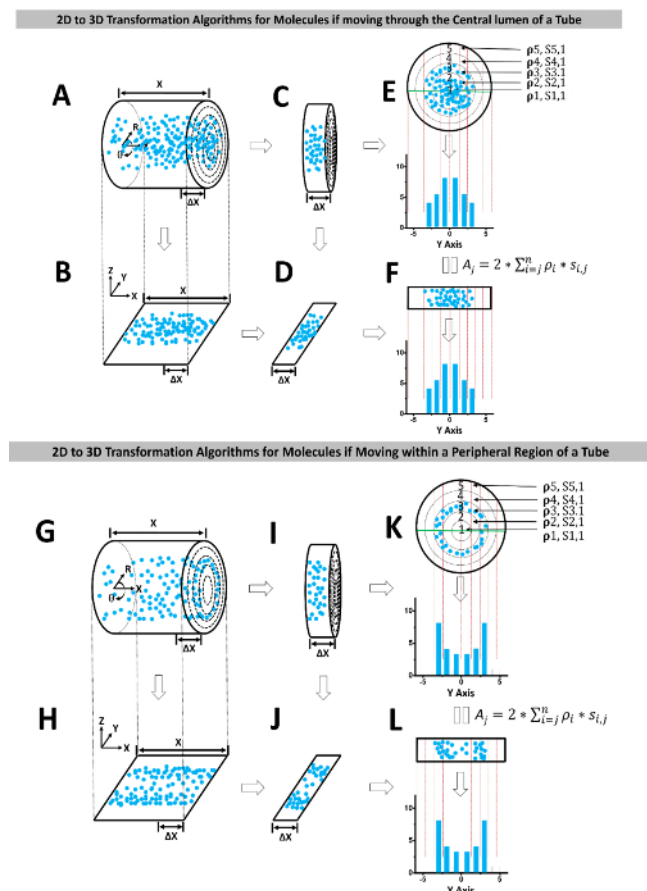
Figure 2. Graphical demonstration of 2D to 3D conversion process. Schematics demonstrate the 2D to 3D transformation algorithm for molecules, for example, if they diffuse within the central lumen (A-F) or a peripheral region (G-L) of a tube. (A) Ideal 3D spatial locations of randomly diffusing molecules inside a tube can be coordinated in a cylindrical coordination system (R, X, θ). In SPEED, only the 3D density map is ultimately calculated from the 2D spatial locations. However, this is an idealized case to illustrate that the 3D density map is equivalent whether the 2D or 3D spatial locations are known. (B) The 3D molecular locations in A are projected onto a 2D plane in a Cartesian coordination system (X, Y, Z) by microscopy imaging. (C) A very thin slice (Δx) cut from the cylinder in A along x dimension. (D) The 3D spatial locations in the slice shown in C can be projected within a narrow 2D region. (E) Cross-section view of all the locations in the thin slice shown in C. These locations can be grouped into the sub-regions between concentric rings. Given the high-number randomly distributed molecules in the cylinder and the cut very thin slice, the spatial density of locations (p_i) in each sub-region (S_i) between two neighboring rings will be rotationally symmetrical and uniform. These locations can be further projected into 1D along the Y dimension. If the locations along Y dimension are clustered in a histogram with j columns. The total number of locations in each column (A_j) is equal to $2 * \sum_{i=j}^{n} \rho_i * s_{i,j}$, which can be experimentally measured as shown in (F). (G-L) Similar as the above, the transformation process is presented for molecules diffusing within a peripheral region of a tube. Please click here to view a larger version of this figure.
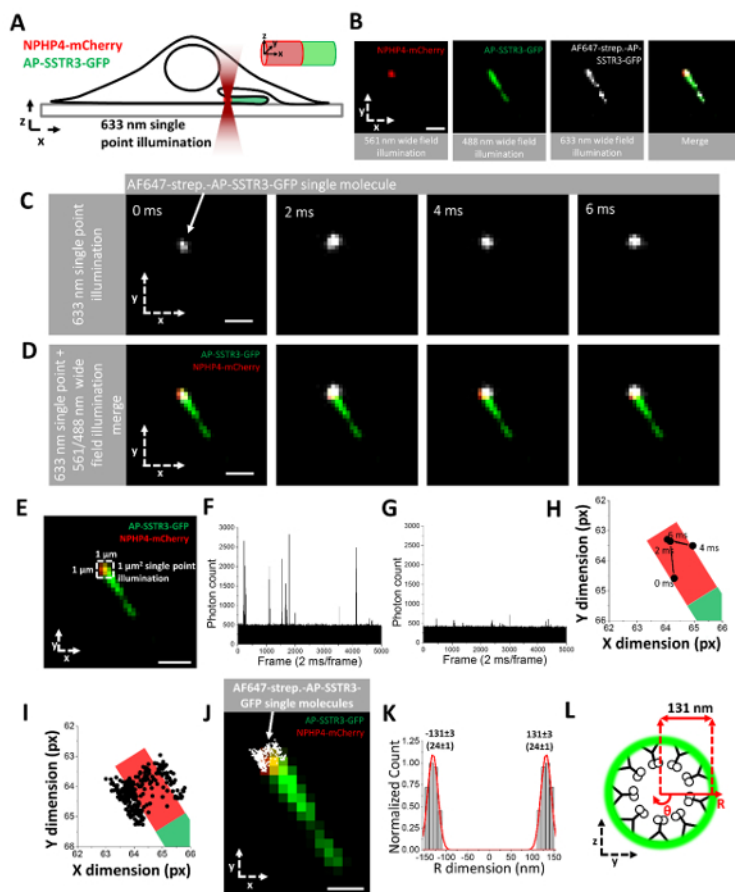
Figure 3. 3D spatial location of the transport route for SSTR3 on live primary cilia mapped by SPEED microscopy. (A) Graphical representation of SPEED microscopy being applied to tracking of GFP-tagged SSTR3 through the TZ marked by NPHP4-mCherry. (B) Epifluorescence image of NPHP4-mCherry (red), AP-SSTR3-GFP (green), Alexa647 used to externally label AP-SSTR3-GFP (white), and the final merged image. Scale bar: 2 µm. (C) Tracking of a single Alexa 647-labeled AP-SSTR3-GFP (white) that passes through the point illumination field for four frames (2 ms/frame). Scale bar: 2 µm. (D) Single molecule trajectory (white) from (C) superimposed on the epifluorescence image of NPHP4-mCherry (red) and AP-SSTR3-GFP (green). Scale bar: 2 µm. (E) White dashed square highlights the area of single point illumination centered on the TZ. Scale bar: 2 µm. (F) Photon count vs Frame number graph for a single molecule video with a high signal to noise ratio determined by dividing the maximum fluorescence of the single molecule divided by the background fluorescence. (G) Photon count vs Frame number graph for a single molecule video with a low signal to noise ratio. (H) Trajectory from (E) and (D) localized in each frame by 2D Gaussian fitting and superimposed on an accurate graphical representation of the TZ, also localized by 2D Gaussian fitting. The 2D Gaussian fitting process fits a Gaussian function to the X and Y dimensions of the intensity profile of an area of interest (AOI) encompassing the single molecule's PSF.(I) 2D super-resolution spatial distribution of 220 individual Alexa Fluor 647-labeled AP-SSTR3-GFP locations collected from a single primary cilium. (J) Super-resolution single molecule locations from (I) superimposed on the epifluorescence image of NPHP4-mCherry (red) and AP-SSTR3-GFP (green). Scale bar: 2 µm. (K) By a 2D to 3D transformation algorithm, the spatial probability density distribution of Alexa Fluor 647-labeled AP-SSTR3-GFP on primary cilia along the R dimension was obtained. Based on Gaussian function fitting, Alexa Fluor 647-labeled AP-SSTR3-GFP primarily located on the ciliary membrane at a radius of 131±3 nm with a full width at half maximum (FWHM) of 24±1 nm. (L) Cross-section view of the spatial probability density distribution (green cloud) of Alexa Fluor 647-labeled AP-SSTR3-GFP on primary cilia. Please click here to view a larger version of this figure.
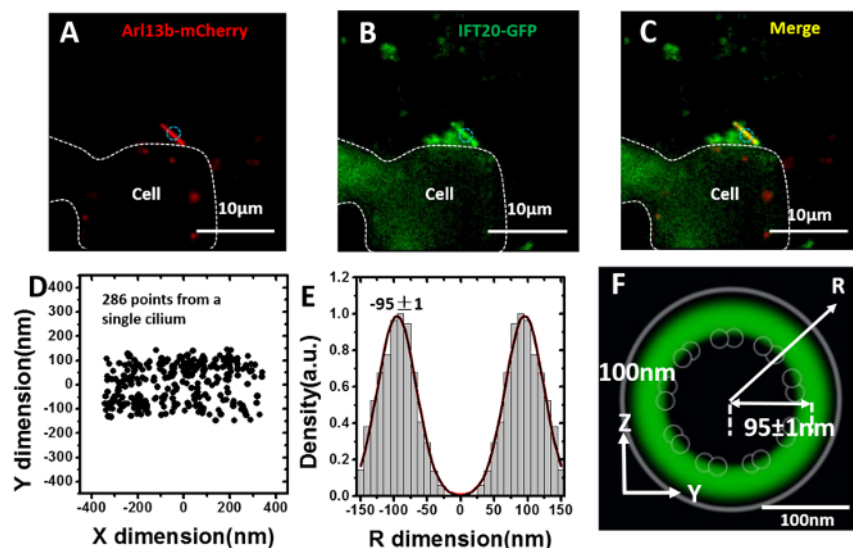
Figure 4. 3D spatial location of the transport route for IFT20 inside live primary cilia mapped by SPEED microscopy. (A-C) Representative image of Arl13b-mCherry (A) and IFT20-GFP (B) co-expressed in an NIH3T3 cell and the merged (C). The circle (cyan) indicates the location of single-point illumination of SPEED microscopy on a primary cilium grew on the side of a cell (white dashed lines) whose edges are determined by IFT20-GFP fluorescence in the cell body and bright field illumination (not shown). Scale bar: 10 µm. (D) 2D super-resolution spatial distribution of 286 individual IFT20-GFP locations collected from a single primary cilium. (E) By a 2D to 3D transformation algorithm, the spatial probability density distribution of IFT20-GFP inside primary cilia along the R dimension is obtained. Based on Gaussian function fitting, IFT20-GFP primarily locate at a radius of 95±1 nm with a full width at half maximum (FWHM) of 56±5 nm. (F) Cross-section view of the spatial probability density distribution (green clouds) of IFT20-GFP in primary cilia, overlaid with the schematic in H. Scale bar: 100 nm. Please click here to view a larger version of this figure.
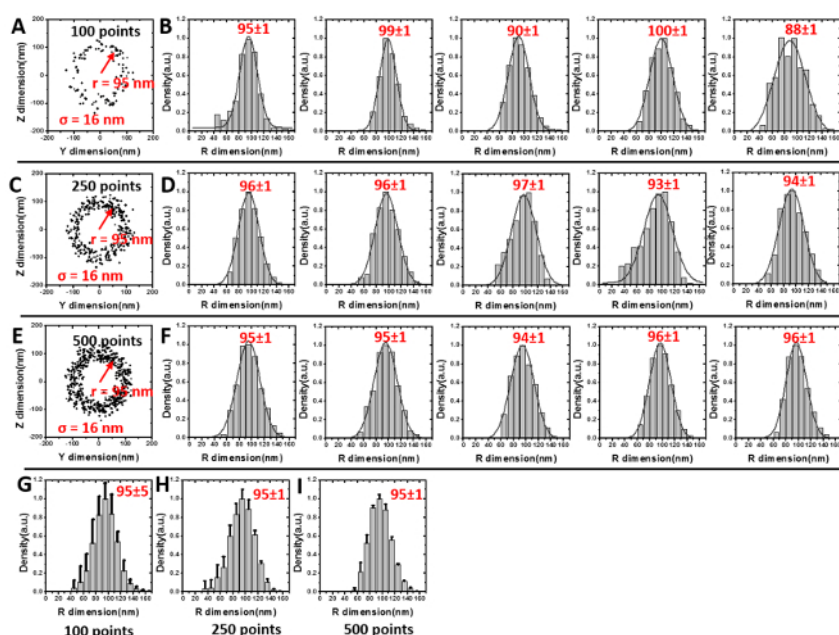

Figure 5. Simulation was used to estimate the minimum number of 2D single-molecule locations to generate a reliable 3D spatial probability density map for the 2D to 3D transformation algorithms. (A) 100 computationally-generated single-molecule locations randomly sample from a radial density normal distribution centered at 95 nm (corresponding to the primary transport route of IFT20 determined in our experiments). Localization precision of 16 nm is simulated for each single-molecule location by sampling from a normal distribution with σ = 16 nm. As shown in **Figure 2C**, a very thin slice (Δx) in the X dimension is used for transformation algorithms and therefore the X dimension is not shown in the computationally-generated 2D single-molecule locations. (B) Transformation between Y-dimensional project data and 3D R-dimensional density generate histograms of 3D R-dimensional densities for five different simulated data sets (each with 100 points). The number above is the peak position ± fitting error. (C-D) Simulation results based on 250 single-molecule locations. (E-F) Simulation results based on 500 single-molecule locations. (G-I) Average 3D density histograms from 100-, 250- and 500-points simulations respectively. Error bars represent variability in the histogram bin heights while the number above the peak is the average peak position ± standard deviation. Please click here to view a larger version of this figure.

Discussion

This protocol describes the application of SPEED microscopy to the primary cilium, a cellular signaling organelle that is highly reliant on efficient protein transport. SPEED microscopy can provide high resolution (< 10 nm) locations for fluorescently-labeled molecules as they pass through the single point illumination centered on the TZ. Previously it has been applied to study the protein trafficking through the NPC[6,7,8]. However, it may be extended to study trafficking through any sub-diffraction cellular cavity. This technique has an advantage over other high-resolution imaging techniques in that it is able to capture the dynamics of single protein transport in live cell systems at a spatial and temporal resolution of <10 nm and <2 ms, respectively. Another advantage is that one must only fluorescently-label a protein of interest and express the construct via transfection, a common molecular biology approach to studying protein localization, to begin performing SPEED microscopy. One must keep in mind that the single point illumination with a high-power laser is the feature that provides the well-separated, high resolution single molecule locations. However, this also limits the illumination area and makes the technique not suitable for wide field localization. Fortunately, there are many wide field super resolution techniques for investigators to choose from if desired. Another point to consider is that SPEED microscopy only captures locations of moving single molecules. Therefore, combination with FRAP, which can determine the fraction of total molecules that are mobile, may be a useful addition to analysis.

The conversion process between the Cartesian and the cylindrical coordination system is to generate a virtual 3D probability density map rather than a 3D view based on 3D single-molecule tracking. In detail, electron microscopy data have revealed that the primary cilia have a rotationally symmetrical structure which could generate a uniform molecule distribution along certain radius. This uniform distribution leads that the spatial distribution along θ dimension in the cylindrical system is constant. Then the 3D coordinates (R, X, θ) can be simplified to be the 2D coordinates (R, X, constant). Actually, our transform process between the Cartesian and the cylindrical systems is from 2D (X, Y) to 2D (R, X, constant). The constant θ, refers to the spatial density p, is calculated by using the equation $Aj = 2 * \sum_{i=j}^{n} \rho_i * s_{i,j}$ (**Figure 2**). Use a matrix calculator to calculate the vector $s_{i,j}$, which corresponds with the relative areas between neighboring concentric rings in the cross-section view[6,7] Aj s the total interaction sites at the position j measured directly from experiments; Thus, pi, the spatial probability density of the interaction sites at r$_i$, can be calculated by solving the matrix equation of $Aj = 2 * \sum_{i=j}^{n} \rho_i * s_{i,j}$.

A critical step in the protocol is to minimize any perturbation of the microscopy setup between the reference image acquisition and single molecule video. If any movement occurs, it is not possible to confidently map the single molecule locations to the ultrastructure of the primary cilia that was obtained via epifluorescence imaging. Another essential step is to photobleach the area of illumination enough to locally reduce the concentration of fluorescently labeled single molecules but not so much that the population is completely photobleached. In the case of SSTR3, the diffusion coefficient is slow compared to soluble molecules and the movement of a population of un-photobleached SSTR3 molecules back into the photobleached area will be longer than two minutes, the time beyond which the ciliary drift is a non-negligible factor. If the proper level of photobleaching is difficult to attain and a high level of background fluorescence is still present, an angled illumination laser may be used to reduce the amount of fluorescently labeled single molecules that are excited above and below the imaging plane. This will reduce the background and improve the signal-to-noise ratio for each captured single molecule.

In summary, SPEED microscopy is able to be readily implemented on conventional microscopy setups by the addition of a laser illumination source, associated mirrors, and high speed CCD camera. The main advancement over other similar techniques are the inclined laser which greatly reduces the background fluorescence and the 2D-to-3D transformation algorithm which reconstructs the 3D spatial probability density map from the 2D single-molecule locations. From a biological standpoint, no extra labeling besides a fluorophore-conjugated protein of interest is needed. These features allow SPEED microscopy to track single molecules with high spatiotemporal (5-10 nm, 0.4-2 ms) resolution as they traffic through a sub-micrometer bio-cavity or bio-channel with rotationally symmetric structures. Coupled with a 3D probability density transformation algorithm, the 3D transport routes of the tagged proteins may be determined through the cavity or channel. The application of this technique has been previously used to distinguish 3D transport routes of proteins and RNAs through the NPC and, here, we show that the 3D transport of a transmembrane protein, SSTR3, and a cytosolic protein, IFT20, may be achieved in the TZ of primary cilia. Other super resolution techniques, such as 3D-STORM, have obtained x,y,z positions for single molecules by placing a cylindrical lens in the optical path which creates an asymmetrical distortion of the single-molecule PSF depending on its position above or below the focal plane[28]. Another advance may attempt to implement virtual pinhole technology to reduce the width of the emission PSF and thus increase resolution even further. The above techniques could be implemented on SPEED microscopy quite readily. Overall, SPEED microscopy provides a unique approach in simultaneously determining transport kinetics at single-molecule level and 3D map of transport pathways with super-high spatiotemporal resolution for inter- or intra-organelle molecular trafficking under certain circumstances in live cell systems.

Disclosures

The authors declare no conflicts of interest.

Acknowledgements

References

1. Huang, B., Bates, M., & Zhuang, X. Super-resolution fluorescence microscopy. *Annu Rev Biochem*. **78**, 993-1016 (2009).
2. Leung, B. O., & Chou, K. C. Review of super-resolution fluorescence microscopy for biology. *Appl Spectrosc*. **65**, 967-980 (2011).

3. Willig, K. I., Rizzoli, S. O., Westphal, V., Jahn, R., & Hell, S. W. STED microscopy reveals that synaptotagmin remains clustered after synaptic vesicle exocytosis. *Nature.* **440**, 935-939 (2006).
4. Betzig, E. *et al.* Imaging intracellular fluorescent proteins at nanometer resolution. *Science.* **313**, 1642-1645 (2006).
5. Rust, M. J., Bates, M., & Zhuang, X. Sub-diffraction-limit imaging by stochastic optical reconstruction microscopy (STORM). *Nat Meth.* **3**, 793-796 (2006).
6. Ma, J., & Yang, W. Three-dimensional distribution of transient interactions in the nuclear pore complex obtained from single-molecule snapshots. *Proc Natl Acad Sci USA.* **107**, 7305-7310 (2010).
7. Ma, J., Goryaynov, A., Sarma, A., & Yang, W. Self-regulated viscous channel in the nuclear pore complex. *Proc Natl Acad Sci USA.* **109**, 7326-7331 (2012).
8. Ma, J. *et al.* High-resolution three-dimensional mapping of mRNA export through the nuclear pore. *Nat Comm.* **4** (2013).
9. Akey, C. W., & Radermacher, M. Architecture of the Xenopus nuclear pore complex revealed by three-dimensional cryo-electron microscopy. *J Cell Biol.* **122**, 1-19 (1993).
10. Akey, C. W. Interactions and structure of the nuclear pore complex revealed by cryo-electron microscopy. *J Cell Biol.* **109**, 955-970 (1989).
11. Czarnecki, P. G., & Shah, J. V. The ciliary transition zone: from morphology and molecules to medicine. *Trends Cell Biol.* **22**, 201-210 (2012).
12. Elf, J., Li, G.-W., & Xie, X. S. Probing transcription factor dynamics at the single-molecule level in a living cell. *Science.* **316**, 1191-1194 (2007).
13. Anzalone, A., Annibale, P., & Gratton, E. 3D orbital tracking in a modified two-photon microscope: an application to the tracking of intracellular vesicles. *J Vis Exp.* (2014).
14. Ritter, J. G., Veith, R., Veenendaal, A., Siebrasse, J. P., & Kubitscheck, U. Light sheet microscopy for single molecule tracking in living tissue. *PloS one.* **5**, e11639 (2010).
15. Marshall, W. F., & Nonaka, S. Cilia: tuning in to the cell's antenna. *Curr Biol.* **16**, R604-R614 (2006).
16. Scholey, J. M., & Anderson, K. V. Intraflagellar transport and cilium-based signaling. *Cell.* **125**, 439-442 (2006).
17. Yang, T. T. *et al.* Superresolution pattern recognition reveals the architectural map of the ciliary transition zone. *Sci Rep.* **5**, 14096 (2015).
18. Craige, B. *et al.* CEP290 tethers flagellar transition zone microtubules to the membrane and regulates flagellar protein content. *J Cell Biol.* **190**, 927-940 (2010).
19. Kee, H. L. *et al.* A size-exclusion permeability barrier and nucleoporins characterize a ciliary pore complex that regulates transport into cilia. *Nat Cell Biol.* **14**, 431-437 (2012).
20. Najafi, M., Maza, N. A., & Calvert, P. D. Steric volume exclusion sets soluble protein concentrations in photoreceptor sensory cilia. *Proc Natl Acad Sci USA.* **109**, 203-208 (2012).
21. Nachury, M. V., Seeley, E. S., & Jin, H. Trafficking to the ciliary membrane: how to get across the periciliary diffusion barrier? *Annu Rev Cell Dev Biol.* **26**, 59-87 (2010).
22. Ye, F. *et al.* Single molecule imaging reveals a major role for diffusion in the exploration of ciliary space by signaling receptors. *Elife.* **2**, e00654 (2013).
23. Ross, A. J. *et al.* Disruption of Bardet-Biedl syndrome ciliary proteins perturbs planar cell polarity in vertebrates. *Nat Genetics.* **37**, 1135-1140 (2005).
24. Selective targeting of somatostatin receptor 3 to neuronal cilia. *Neuroscience.* **89**, 909-926 (1999).
25. Follit, J. A., Tuft, R. A., Fogarty, K. E., & Pazour, G. J. The intraflagellar transport protein IFT20 is associated with the Golgi complex and is required for cilia assembly. *Mol Biol Cell.* **17**, 3781-3792 (2006).
26. Awata, J. *et al.* NPHP4 controls ciliary trafficking of membrane proteins and large soluble proteins at the transition zone. *J Cell Sci.* **127**, 4714-4727 (2014).
27. Howarth, M., & Ting, A. Y. Imaging proteins in live mammalian cells with biotin ligase and monovalent streptavidin. *Nat Protoc.* **3**, 534-545 (2008).
28. Huang, B., Wang, W., Bates, M., Zhuang, X. Three-dimensional super-resolution imaging by stochastic optical reconstruction microscopy. *Science.* **319**, 810-813 (2008).